



Invited Article

Metal Fuel Development and Verification for Prototype Generation IV Sodium-Cooled Fast Reactor



Chan Bock Lee*, Jin Sik Cheon, Sung Ho Kim, Jeong-Yong Park, and Hyung-Kook Joo

Korea Atomic Energy Research Institute, 989-111 Daedeok-daero, Yuseong-gu, Daejeon, South Korea

ARTICLE INFO

Article history:

Received 10 August 2016

Accepted 17 August 2016

Available online 24 August 2016

Keywords:

Ferritic–Martensitic Steel

Irradiation Test

Metal Fuel

Pyroelectrochemical

Sodium-cooled Fast Reactor

Spent Fuel

Transuranic Fuel

ABSTRACT

Metal fuel is being developed for the prototype generation-IV sodium-cooled fast reactor (PGSFR) to be built by 2028. U–Zr fuel is a driver for the initial core of the PGSFR, and U–transuramics (TRU)–Zr fuel will gradually replace U–Zr fuel through its qualification in the PGSFR. Based on the vast worldwide experiences of U–Zr fuel, work on U–Zr fuel is focused on fuel design, fabrication of fuel components, and fuel verification tests. U–TRU–Zr fuel uses TRU recovered through pyroelectrochemical processing of spent PWR (pressurized water reactor) fuels, which contains highly radioactive minor actinides and chemically active lanthanide or rare earth elements as carryover impurities. An advanced fuel slug casting system, which can prevent vaporization of volatile elements through a control of the atmospheric pressure of the casting chamber and also deal with chemically active lanthanide elements using protective coatings in the casting crucible, was developed. Fuel cladding of the ferritic–martensitic steel FC92, which has higher mechanical strength at a high temperature than conventional HT9 cladding, was developed and fabricated, and is being irradiated in the fast reactor.

Copyright © 2016, Published by Elsevier Korea LLC on behalf of Korean Nuclear Society. This is an open access article under the CC BY-NC-ND license (<http://creativecommons.org/licenses/by-nc-nd/4.0/>).

1. Introduction

A prototype generation-IV sodium-cooled fast reactor (PGSFR) is being developed in combination with the pyroelectrochemical processing of spent PWR fuel, as shown in Fig. 1. U–Zr fuel is a driver for the initial core of the PGSFR, and U–transuramics (TRU)–Zr fuel will gradually replace U–Zr fuel through its qualification in the PGSFR. The pyroelectrochemical

processing extracts uranium and TRU, and separates fission products for disposal from the spent fuel. The extracted uranium and TRU, including Pu and long-lived minor actinides such as Np, Am, and Cm, are used to fabricate the U–TRU–Zr metal fuel. This fuel recycling can solve the problem of PWR spent fuel accumulation by reducing the volume of PWR spent fuel and can increase the utilization of uranium resources while maintaining high proliferation resistance [1,2].

* Corresponding author.

E-mail address: cblee@kaeri.re.kr (C.B. Lee).
<http://dx.doi.org/10.1016/j.net.2016.08.001>

1738-5733/Copyright © 2016, Published by Elsevier Korea LLC on behalf of Korean Nuclear Society. This is an open access article under the CC BY-NC-ND license (<http://creativecommons.org/licenses/by-nc-nd/4.0/>).

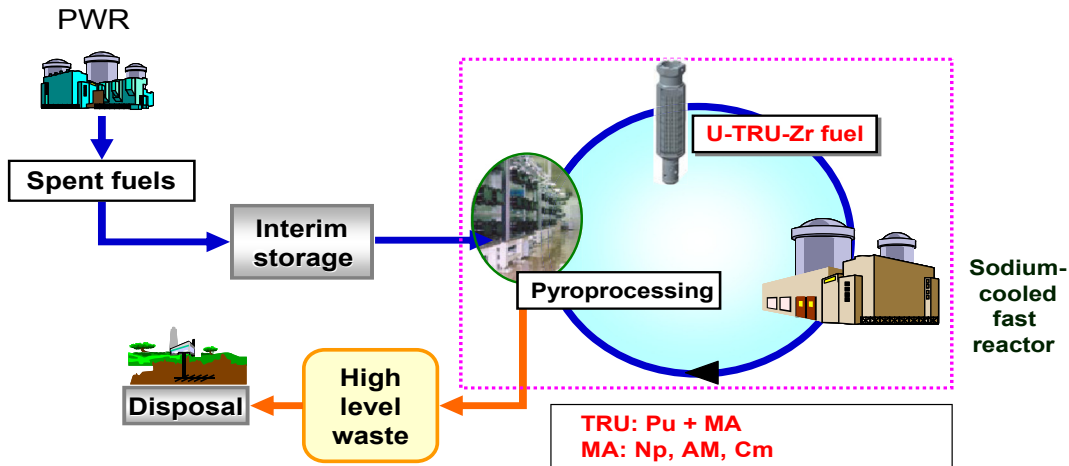


Fig. 1 – SFR pyroelectrochemical fuel recycling. MA, minor actinides; PWR, pressurized water reactor; SFR, sodium-cooled fast reactor; TRU, transuranics.

Higher thermal conductivity of metal fuel and adoption of a fuel design with a sodium fuel gap can keep the fuel temperature low during irradiation. Metal fuel has noble compatibility with a sodium reactor coolant, which guarantees flexibility and a margin during reactor operation [3–6]. Therefore, an SFR using metal fuel can be operated with passive safety, which implies that fuel integrity is maintained during transients without the support of an active reactor cooling system [7]. Technical challenges of recycling TRU metal fuel are remote fuel fabrication in a radioactivity-shielded hot cell and the irradiation performance of TRU metal fuel containing chemically active lanthanide impurities, as well as the development of advanced cladding materials up to high burnup and a high temperature.

This paper summarizes the results of metal fuel development for a PGSFR such as fuel design and evaluation, fuel fabrication, fuel components development and fabrication, and fuel verification tests.

2. Metal fuel development

2.1. Metal fuel design for PGSFR

Metal fuel for a PGSFR was designed as shown in Fig. 2. Metal fuel slugs are encapsulated inside a cladding tube. The fuel gap between the fuel slug and cladding is filled with sodium to enhance heat transport. A wire is wrought on the outer surface of the fuel rod to maintain the gap between fuel rods to allow the sodium coolant to flow. Shielding blocks are located at both ends of the fuel assembly to protect the core internals from irradiation damage.

The fuel pin is fabricated with an upper end cap, a cladding, a lower end cap, and wire. The fuel lattice and pitch are maintained by the wire wrap. The overall length of the fuel rod is 2,240 mm. The diameter and length of fuel slug are 5.54 mm and 900 mm, respectively. The outer diameter of the cladding is 7.4 mm and the cladding thickness is 0.5 mm. The wire diameter is 0.95 mm. Smear density of fuel slug in a fuel rod is

75%. The length of plenum is 1,275 mm, and the initial sodium height above fuel slug is 25 mm.

Bundles of 217 fuel rods are surrounded by a hexagonal duct in a fuel assembly. HT9 was selected as a duct material based on its irradiation experiences in the USA [4]. A hexagonal duct has several functions: to provide a coolant path, support the overall rigidity of the fuel assembly, assemble the fuel rods, and limit a lateral bowing of the fuel assembly. Fuel rods are inserted into the 17 mounting rails, varying from 9 to 17 rods in a row. These mounting rails are inserted in the top region of the lower reflector. In this way, the lower end of the fuel rod is supported and the upper end is free. At the bottom of the fuel assembly, there is a nose piece with nine flow holes through which sodium coolant flows into the fuel assembly. At the top of the fuel assembly, a fuel handling socket is attached for gripping the fuel assembly for transport. There are two load pads to achieve favorable deformation of fuel assemblies from the aspects of reactivity feedback during transients: the top load pad is located at the handling socket, and the above-core load pad is located above the active core. In the handling socket, there are two holes for the handling tool of the refueling machine.

Based on the radiation shielding analysis to protect both lower and upper support structures in the core from radiation damage, the length of the lower shielding block is set as 900 mm and that of the upper shielding block as 500 mm. The total weight of the fuel assembly is about 296 kg.

Fuel assemblies adopt the hydraulic hold-down concept rather than a mechanical clamping device. Sodium inlet holes located on the side of the nose piece acts to eliminate the upward thrust force produced by sodium influx to the assembly. Furthermore, the hydraulic bypass line to the low-pressure zone is located at the bottom of assembly, and counteracts high-pressure sodium at the assembly inlet.

2.2. Fuel fabrication

Metal fuel can be fabricated using a variety of casting methods, out of which injection casting is known to be the most cost

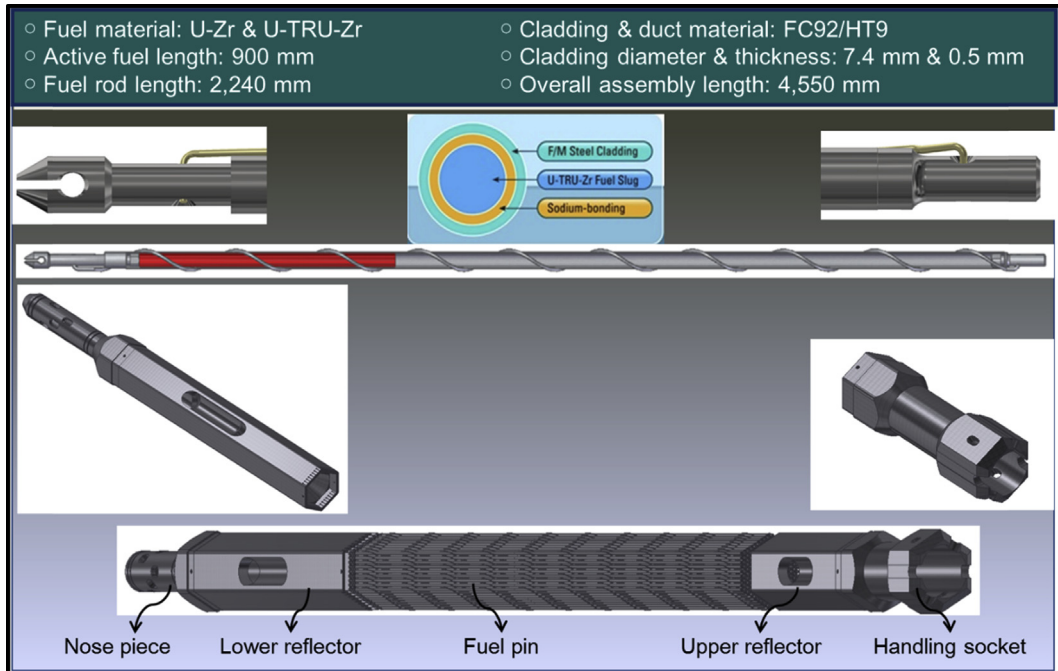


Fig. 2 – PGSFR metal fuel. PGSFR, prototype generation-IV sodium-cooled fast reactor; TRU, transuranics.

efficient, capable of mass production, and suitable for remote operation. A great number of metallic fuel slugs have been fabricated successfully by injection casting to be used as driver and test fuels in the USA [8]. Fig. 3 shows the fabrication process of the metal fuel. Injection casting conditions such as temperature, pressure, pressurizing rate, and mold coating need to be optimized. Dimensions, weight, straightness, relative U-235

enrichment distribution along the axial direction, and chemical contents of fuel slugs are measured after injection casting. Slurry coating with a ceramic material is employed on the inside of the graphite crucible to prevent the chemical reaction between the melt and the crucible. Quartz tubes are used as casting molds of fuel slugs. The casting chamber is maintained under a vacuum of less than 1×10^{-3} Torr during induction

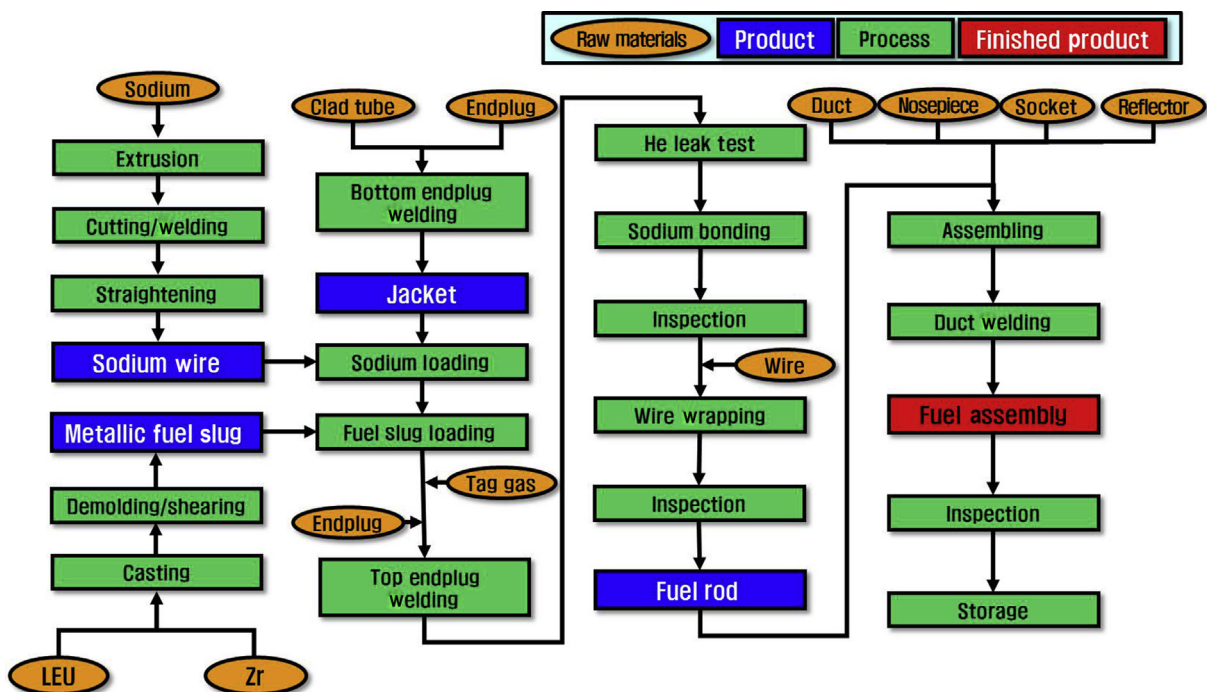


Fig. 3 – Fabrication process of PGSFR metal fuel. PGSFR, prototype generation-IV sodium-cooled fast reactor; LEU, low enriched uranium.

heating with a ramp rate of 100°C/min. Ar gas is applied from the accumulator tank connected to the casting furnace in order to drive the melt into the quartz molds. Fabricated slugs after injection casting are removed from the mold assembly in a glove box.

Solid sodium lump is extruded and inserted into the jacket that is fabricated by welding the cladding tube with the lower end plug. Fuel slugs are placed on the top of the sodium lump in the jacket. After gas tungsten arc welding of the jacket with the upper end plug, sodium bonding is carried out in the gap between the fuel and the cladding tube. The quality of sodium bonding is checked by sodium level, existence of any void, and slug position inside the fuel rod. Welding of the end plugs is qualified through tensile, burst, and helium leak tests. The wire wrapping equipment, which can control the wire pitch, wire tension, and the size of fusion ball at the ends, was developed. Fig. 4 shows the fabricated U–10Zr fuel rods for the irradiation test at the BOR-60 research reactor [9].

In order to fabricate U–TRU–Zr fuel while maintaining the advantages of injection casting, process parameters need to be controlled more precisely under the circumstances that the chemistry and microstructure are significantly influenced by the casting conditions. As the first step toward the development of a novel injection casting method that can be applied to the remote fabrication of U–TRU–Zr fuel, the effect of the process parameters on the chemical and microstructural properties of fuel slugs was investigated to better understand how the volatile constituents behave during the casting process.

Fuel slugs with a nominal composition of U–10 wt% Zr–5 wt% Mn were fabricated. Mn was selected as a surrogate for americium (Am) since its vaporization pressure is comparable with that of Am [10]. The pressurized injection casting method

was developed to fabricate the fuel slug containing volatile elements. Three different pressure conditions (vacuum condition, 400 Torr, and 600 Torr Ar atmosphere) were investigated. During the vacuum condition, 68% of Mn was evaporated. In both pressurized conditions, however, no evaporation of Mn was detected in the chemical composition analysis of the fuel slugs by the ICP-AES (inductively coupled plasma-atomic emission spectroscopy) method.

Injection casting of RE (rare earth element)-containing fuel slugs was also investigated since RE exists as impurities, such as 53 wt% Nd–25 wt% Ce–16 wt% Pr–6 wt% La, in the TRU ingot produced by pyroelectrochemical processing of the spent PWR fuel. Casting temperature, injection pressure, preheating temperature, and holding time were adjusted to derive suitable fabrication process conditions. U–10 wt% Zr–5 wt% RE fuel slugs fabricated by injection casting showed that the distribution of RE precipitates was relatively fine and uniform. However, the reaction between the melt and the crucible was found to be significant in the casting of RE-containing fuel slugs compared with that of U–Zr slugs. To mitigate or prevent the interaction of highly reactive RE with a crucible, several coatings were applied on the inner surface of crucible. Plasma-coated Y_2O_3 showed a promising performance. RE contents left in the fuel slugs tend to increase with an increase in the contents of RE charged, as shown in Fig. 5. It is noted that the RE content became somewhat saturated beyond 5 wt%. The difference between the charged and measured RE contents was attributable to the immiscibility of RE with U and Zr, which possibly prevented a substantial amount of the charged RE from mixing with the U–Zr alloys [11].

In order to examine the behavior of RE elements during casting, compositions in the cross section of the melt residue of U–10 wt% Zr–10 wt% RE were investigated. Scanning electron

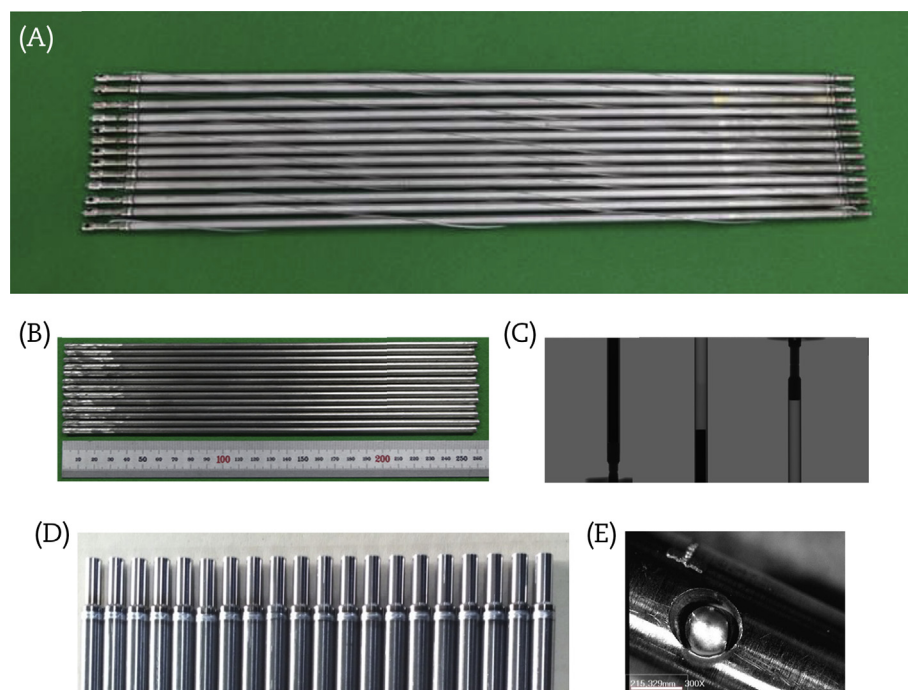


Fig. 4 – Fuel rods for the irradiation test in BOR-60. (A) As-fabricated fuel rods. (B) As-cast fuel slugs. (C) Inspection of sodium bonding with X-ray. (D) End plug welded to cladding. (E) Fused ball at the tip of wire.

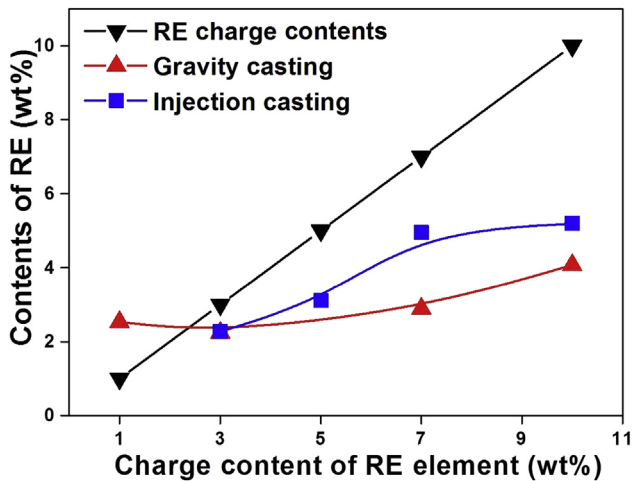


Fig. 5 – Charged and measured contents of RE elements in fuel slug. RE, rare earth.

microscope images in Fig. 6 indicate that there were clear differences in phases between the top layer and the other locations. While chemical composition at the middle of the melt residue was similar to that of fuel slug, the top layer contained RE-rich oxides together with a small amount of yttria. The formation of RE agglomerates in the top layer was considered to be the main reason for the reduced RE content in the melt residue due to the immiscibility of RE with U and Zr [11].

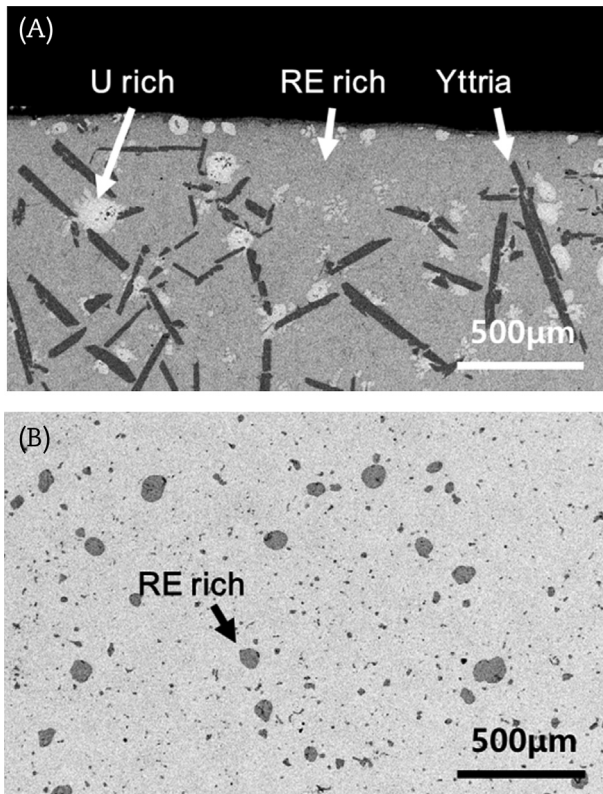


Fig. 6 – Cross-sectional SEM microstructure of the top layer and middle region in the melt residue of the U–10 wt% Zr–10 wt% RE fuel slug. (A) Top layer. (B) Middle region. SEM, scanning electron microscope.

As an innovative method to fabricate U–TRU–Zr fuel, particulate fuels were investigated [12]. Metal fuel particles were fabricated using the centrifugal atomization process. The size of the fuel particles can be controlled in the range of tens to hundreds of microns. The fuel particles can be vibro-packed into the cladding or consolidated through sintering. Another way is that TRU particles can be fabricated directly by utilizing a TRU ingot recovered from pyroelectrochemical processing, and then mixed with particles of uranium and zirconium. This process could alleviate the ingot casting process after TRU recovery by the pyroelectrochemical process. Sodium bonding in a fuel rod may not be needed since a direct contact between the fuel and the cladding can be sustained from the beginning of irradiation. Fig. 7 shows the sintered U–10 wt% Zr fuel pellet and its cross section. Depending on the particle size and sintering conditions of temperature and time, porosity of the sintered fuel pellet can be controlled up to 35%, which is necessary to accommodate the metallic fuel swelling during irradiation.

TRU fuels should be fabricated in a hot cell facility using remote handling equipment since highly radioactive elements are present in the fuel. A remote injection casting equipment was designed as the first step toward developing the remote fabrication equipment for the TRU fuel manufacturing facility. Fig. 8 shows the conceptual design of the remote injection casting equipment. The equipment was designed to

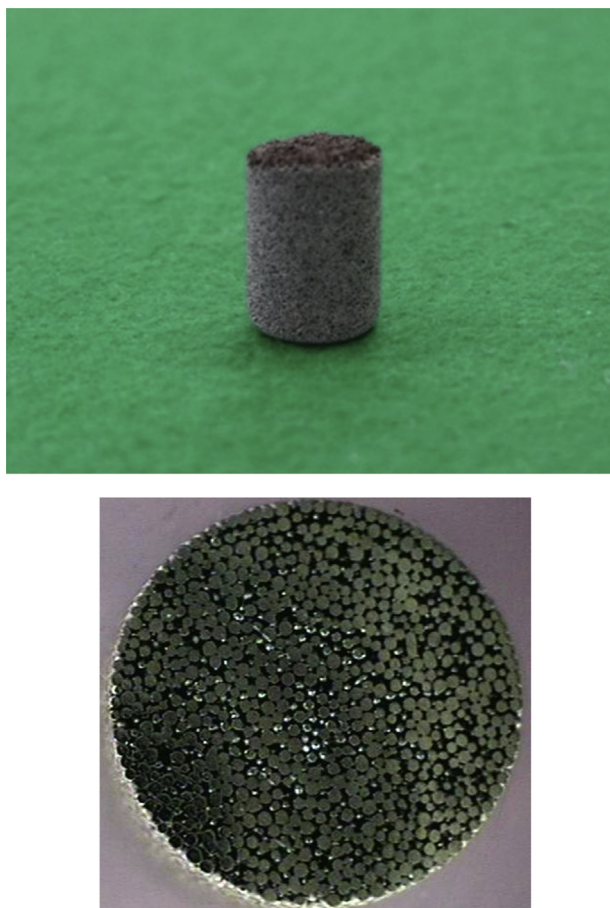


Fig. 7 – Sintered particulate U–10 wt% Zr and its cross section.

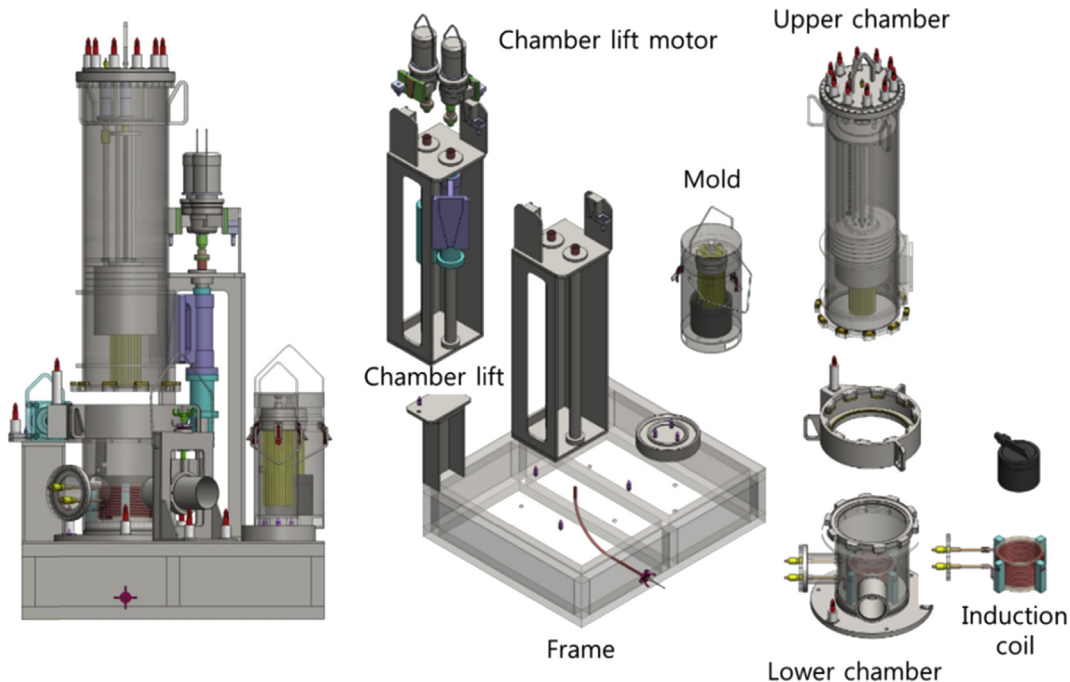


Fig. 8 – Conceptual design of remote injection casting equipment.

accommodate more than 15 kg melt per batch, which is equivalent to more than 50 fuel slugs. The remote injection casting equipment will be installed by the end of 2016 for tests.

2.3. Fabrication and evaluation of fuel components

Ferritic–martensitic (FM) steels have been considered as a primary candidate for the cladding and duct materials of an SFR owing to their higher thermal conductivity, lower thermal expansion, and lower irradiation swelling relative to austenitic stainless steel. HT9 was originally developed for conventional fossil power plants and adopted in the US fast reactor program [13]. It was sufficiently tested as cladding in EBR (experimental breeder reactor)-II, and cladding and duct in FFTF (fast flux test facility) where fuels were MOX (mixed oxide) and metal fuel. HT9 exhibited excellent swelling resistance, which is a prerequisite for a high-burnup application [13] even though it has lower creep strength compared with austenitic stainless steel claddings [14].

New FM steels have been developed by focusing on increasing creep resistance in fossil power plant industries. These activities motivated the introduction of improved FM steels as cladding in SFR fuel development programs [15,16]. The new FM steel claddings have made excellent in-pile records where unexpected issues have not been observed as in the case of HT9 [17,18]. In Russia, FM steels of EK-181 and ChS-139 are being developed for BN-1200 fuel cladding [19]. In Japan, PNC-FMS was chosen as a strong candidate for the cladding material of metal fuel [20]. In India, T91 is being irradiated to be used as fuel cladding in metal fuel of PFBR (prototype fast breeder reactor). Advanced cladding materials called FC92 were developed to cope with a higher core outlet temperature of the PGSFR of 545°C.

An advanced FM steel alloy was developed on the basis of Grade 92 FM steel. Minor alloying elements such as B, Nb, Ta, and C were optimized to achieve better mechanical properties at a high temperature [21]. Thirty-eight alloys were designed for developing advanced cladding materials. Two candidates, FC92B and FC92N, were finalized. Specimens were manufactured by vacuum induction melting, hot rolling, and heat treatment. Fig. 9 shows a comparison of FC92 creep rupture test results at 650°C relative to those of other cladding tube materials. The creep rupture strength of FC92 showed an improvement of above 30% compared with that of HT9 and was comparable to that of other advanced FM steels.

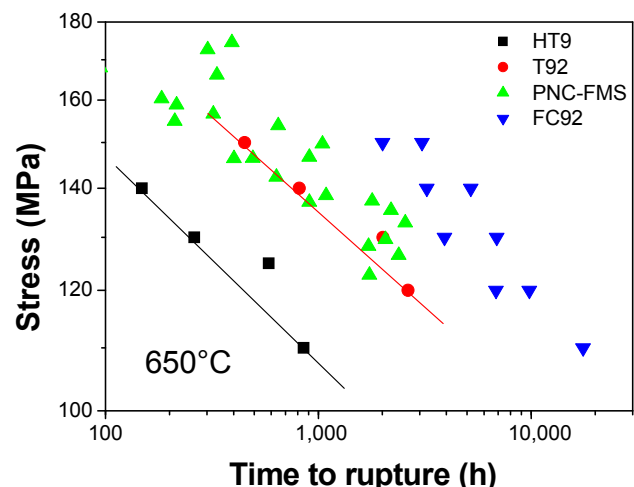


Fig. 9 – Creep rupture strength of FC92 cladding tube material.

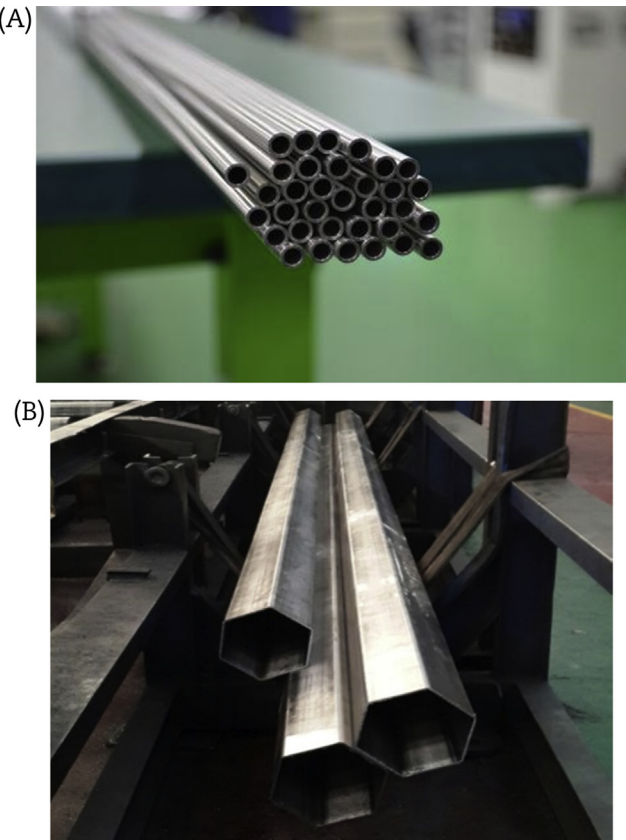


Fig. 10 – Cladding tube and duct. (A) Cladding tube. (B) Duct.

C of FC92 and HT9 (7.4 mm in outer diameter, 0.5 mm in thickness, and 3,000 mm in length) were fabricated as shown in Fig. 10. Cladding is a seamless tube produced by multiple hot/cold working and heat treatments. Dimensional measurements such as outer/inner diameter, thickness, ovality, straightness, and surface roughness have been carried out, which revealed that the final cladding tube satisfied the manufacturing specification. High-temperature mechanical properties such as uniaxial tensile, biaxial burst property, and creep behavior were enhanced by drawing an optimal combination of rolling and heat treatment parameters to attain finer precipitate sizes [22]. Temperature dependency of tensile property of FC92 cladding tube is similar to that of HT9 cladding tube, as shown in Fig. 11.

Cladding tubes of FC92 and HT9 are under irradiation tests in an experimental fast reactor, BOR-60. It is essential not only to demonstrate cladding performance under a fast neutron environment, but also to generate in-pile characteristics data of cladding for fuel design modeling. Irradiation creep and swelling tests are of utmost importance to obtain an in-pile creep model of FC92 for which out-of-pile creep data are used as supplementary information.

Two irradiation rigs were used, Material Test Rig (MTR)-1 and MTR-2, for which nominal irradiation temperatures are 600°C and 650°C, respectively. Irradiation test rigs were designed to be dismantled so that the dimensional changes of irradiated specimens are to be measured during reactor outage periods. Interim inspections through a nondestructive

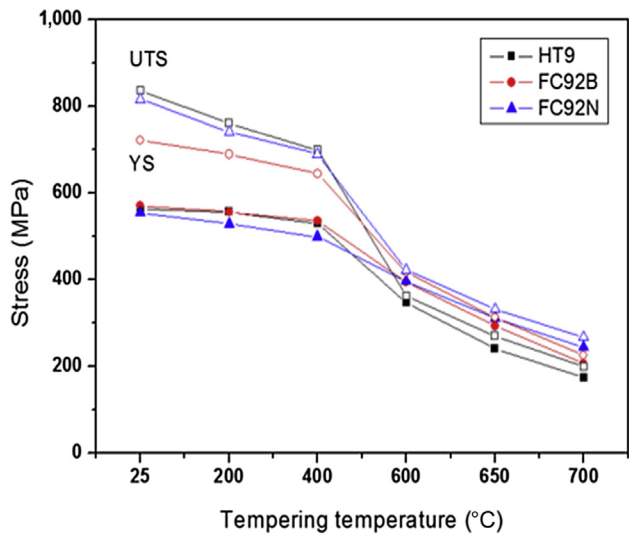


Fig. 11 – Uniaxial tensile test results of cladding tubes. UTS, ultimate tensile strength; YS, yield strength.

way is planned to be made at 15 dpa and 30 dpa for MTR-1 and MTR-2, respectively, and final inspection including destructive tests will be complete in 2020. Each of MTR-1 and MTR-2 contains 36 creep specimens (7.4 mm in diameter and 35 mm in length), 18 swelling specimens (4.57 mm in diameter and 25 mm in length), 72 tensile specimens (with a total length of 25.4 mm), and six microstructure specimens (3 mm in diameter and 25 mm in length). A half of the tensile specimens will be replaced by new ones when each MTR reaches 15 dpa. Fig. 12 shows the irradiation specimens and disassembled parts for MTR-1 and MTR-2.

Target temperatures were achieved by controlling the size of the gap between the rig and the holder housing the irradiation specimens. Tungsten heaters were also placed inside the specimen holders to keep the temperature as flat as possible along the axial direction. Fusion-type temperature monitors and neutron fluence monitors were installed. Since the irradiation test rigs were of noninstrumentation type, their temperatures are affected by a number of parameters such as reactor power, sodium flow rate, specimen orientation, gap thickness, and calculation errors. In-core verification tests of MTR, which were performed in the instrumented channel of BOR-60, enabled us to quantify the uncertainty of irradiation temperature: $600 \pm 16^\circ\text{C}$ for MTR-1 and $650 \pm 15^\circ\text{C}$ for MTR-2.

In March 2015, MTR-1 and MTR-2 tests were initiated after the verification test. As of May 2016, peak irradiation dose reached 12.6 ± 1.5 dpa in MTR-1 and 22.9 ± 0.7 dpa in MTR-2. The first interim inspection was conducted for MTR-2, and irradiation tests are going well.

A hexagonal duct, 132 mm wide \times 4 m long \times 3 mm thick, was fabricated through the processes of ingot melting, piercing, and drawing of a cylindrical tube followed by duct forming, as shown in Fig. 10. Visual inspection as well as dimensional measurements, such as measurements of inter-spacing distance, distortion, and straightness, has been carried out over the manufactured HT9 duct. Tensile tests for the



Fig. 12 – Irradiated specimens and disassembled parts for MTR-1 and MTR-2. MTR, material test rig.

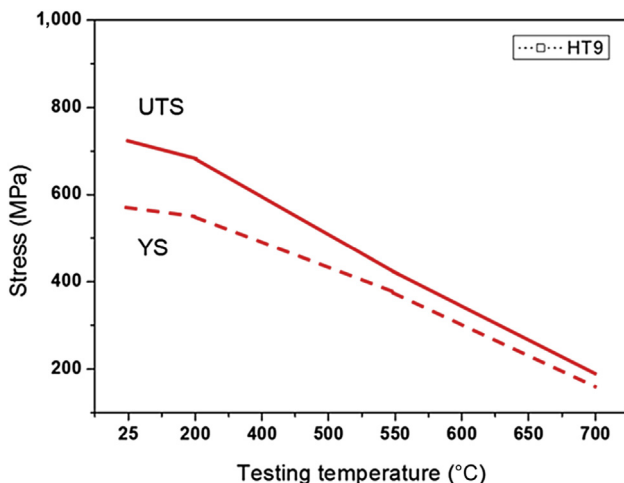


Fig. 13 – Tensile property of HT9 duct.

duct specimens were performed from room temperature to 700°C (Fig. 13).

Impact property of the HT9 duct has been measured. Owing to the thickness limitation of a hexagonal duct, standard Charpy impact specimens were machined from the HT9 cylindrical billet, which was subjected to the final heat treatment same as that of a hexagonal duct. Impact tests were performed in the temperature range of -100°C to 200. Fig. 14 shows the variation of impact energy of the HT9 duct material with temperature, which has been shown to be dependent on specimen orientation, which might be attributed to the orientation of delta ferrites.

2.4. Fuel performance evaluation and verification tests

The PGSFR fuel rod is designed to satisfy its functional and operational requirements for which fuel design criteria have been established. The fuel system damage mechanisms depend on a few key physical phenomena: (1) mechanical deformation of the cladding, (2) cladding wastage, and (3) fuel melting. Among them, cladding wastage for the U-Zr fuel system is not regarded to result directly in a fuel failure, but is one of the phenomena that deteriorate fuel integrity. In addition, fuel melting is primarily adopted since it has traditionally been used as a design criterion in the oxide fuel application. Fuel design criteria were derived for cladding

strain and cumulative damage fraction to avoid fuel failure caused by mechanical deformation of the cladding.

To demonstrate whether each design criterion is satisfied for all the rods of the core at any time, a fuel performance code is employed together with a fuel design methodology, which specifies how to use the code for a design analysis. The fuel design methodology ensures a fuel design procedure enough to have a suitable margin by introducing conservatism by means of uncertainties. The uncertainties are reflected in fuel performance models, fuel rod tolerances, neutronic and thermohydraulic conditions, and plenum volume. The root mean square method is employed to combine the individual effects caused by these uncertainties. The degree of conservatism in the design methodology has been evaluated through an integral analysis using fuel irradiation data. EBR-II X447 [23], and FFTF MFF (mechanistic fuel failure)-3 and MFF-5 [24] data were used. These are most relevant to the PGSFR fuel design in terms of cladding temperature. Peak inner-wall cladding temperatures during irradiation were reported to be 630–660°C for X447, 643°C for MFF-3, and 649°C for MFF-5. During EBR-II X447 tests, two out of 15 sibling fuel rods have failed. By contrast, all the fuel rods of the FFTF MFF series remained intact by increasing the plenum volume relative to the X447 experiment. Design analysis predicts that EBR-X447 fuels fail and that FFTF MFF-3 and MFF-5 fuels are intact, indicating that reasonable conservatism is assigned in the current methodology.

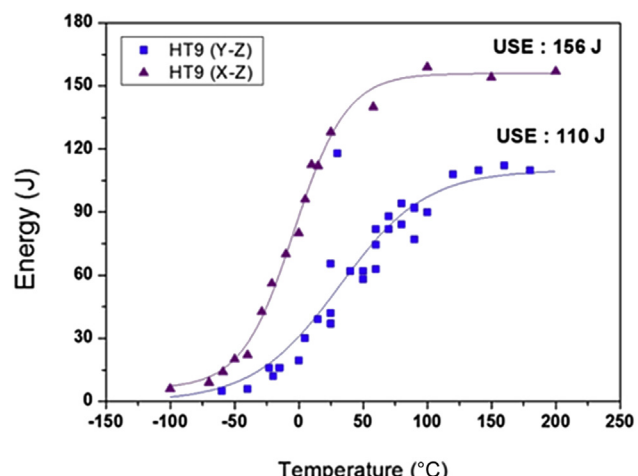


Fig. 14 – Impact property of HT9 duct.

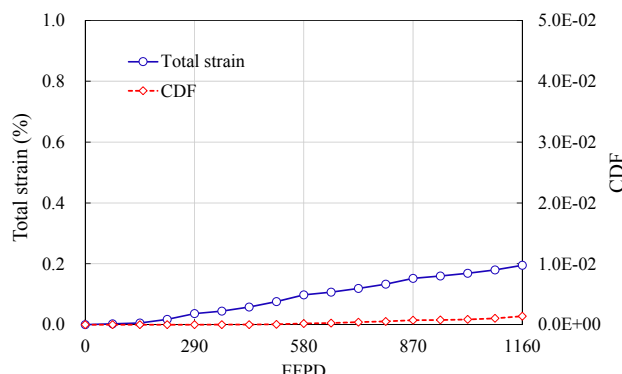


Fig. 15 – Design analysis results of PGSFR fuel rod. CDF, cumulative damage fraction; EFPD, effective full power day; PGSFR, prototype generation-IV sodium-cooled fast reactor.

By applying the fuel design methodology, fuel design analysis was carried out. The PGSFR fuel rod consists of U–10Zr fuel slug and FC92 cladding. Under the equilibrium and nonequilibrium core conditions, analysis results showed that fuel rod design parameters are well below the design criteria of cladding creep strain and CDF (cumulative damage fraction), as shown in Fig. 15.

PGSFR fuel verification is being carried out through in-pile and out-of-pile tests. Irradiation tests of fuel rods and fuel components are underway in both thermal and fast research reactors. Fuel behavior depending on temperature and fission, except fast neutron flux, can be evaluated by irradiation test in thermal reactors such as HANARO Korea atomic energy research institute (KAERI) and advance test reactor (ATR) Idaho national laboratory (INL). Irradiation test in a fast reactor can be conducted in a fast research reactor such as BOR-60 state scientific center-research institute of atomic reactors (RIAR).

Cladding of metal fuel can suffer from fuel cladding chemical interaction (FCCI) by interdiffusion or eutectic melting during irradiation. As the cladding thickness decreases gradually with fuel burnup or might be reduced during

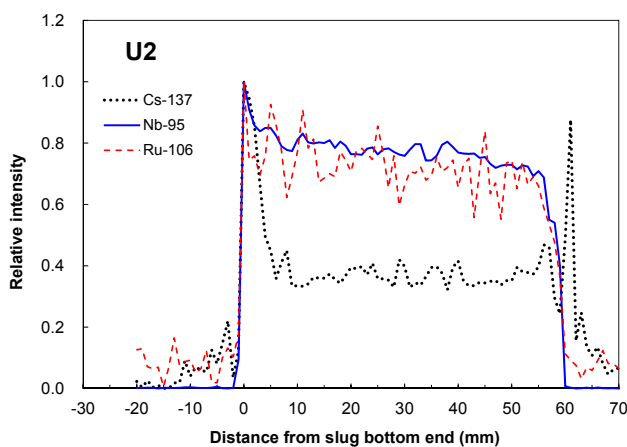


Fig. 16 – Axial gamma scanning from the bottom of U–Zr–5Ce fuel rod.

short transient, the integrity of a fuel rod can be affected. Lanthanide or rare earth fission products can migrate toward fuel outer surface and interact with the cladding. To prevent or retard FCCI, barriers such as Cr electroplating on the inner surface of cladding, oxidation or passivation of either cladding inner surface or outer surface of fuel slug, and duplex cladding with an inner barrier cladding have been investigated.

In 2012, the metal first fuel irradiation test, SFR Metal fuel Irradiation test Program (SMIRP)-1, was performed for 182 EFPD (effective full power day) in HANARO [25]. There were 12 rodlets consisting of six U–10% Zr and six U–10% Zr–5% Ce slugs with T92 cladding. Among them, four rodlets had the cladding with an electroplated Cr barrier of about 20 μm thickness.

The maximum linear power and burnup were calculated to be 245 W/cm at BOL (beginning of life) and 2.87 at% at EOL (end of life), according to an as-run analysis. SMIRP-1 fuels were calculated to be irradiated in the $\alpha + \delta$ regime, which was confirmed by microstructural observation. As shown in Fig. 16, gamma scanning results showed that the axial burnup distribution was more or less uniform with local variations in the microstructure and composition, and that there was a slightly higher axial growth than the previous experience. In addition, fractional fission gas release and fuel constituent

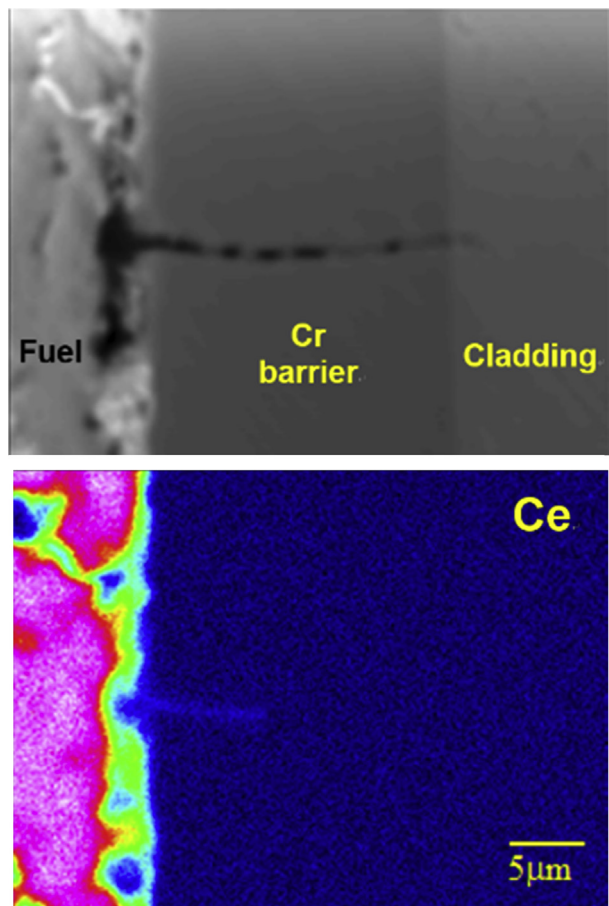


Fig. 17 – SEM image and EPMA map at fuel–cladding interface for U–Zr–5Ce. EPMA, electron probe microanalysis; SEM, scanning electron microscope.

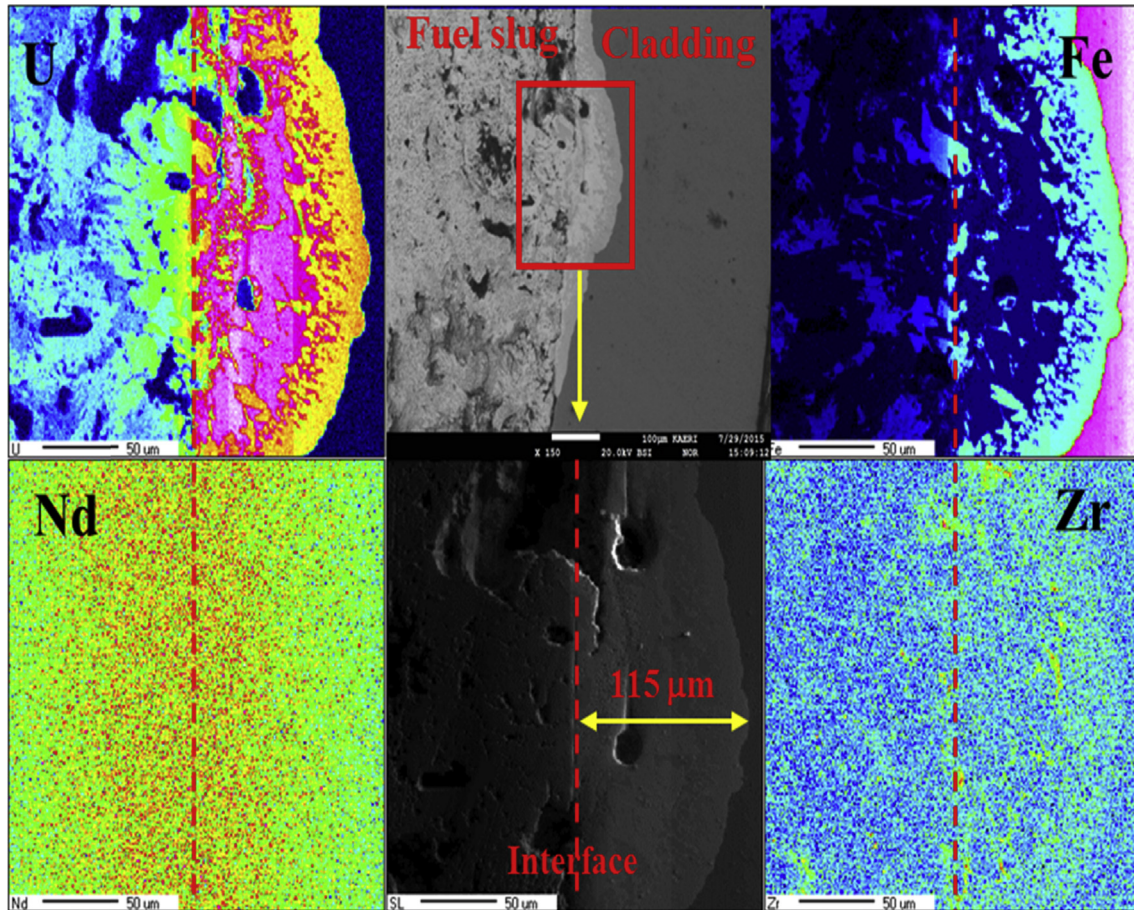


Fig. 18 – Constituent distributions of U–10Zr/T92 specimen after heating test (750°C, 1 h).

redistribution were consistent with the current understanding. Fig. 17 shows that the Cr barrier was excellent at protecting Ce diffusion into the cladding, although the test was performed at a lower temperature [26].

The second irradiation test, SMIRP-2, is under preparation. The SMIRP-2 test extends the irradiation condition of the SMIRP-1 test in terms of temperature, linear power, and

burnup. There are also 12 rodlets with two kinds of fuel slugs, U–10% Zr and U–10% Zr–4% RE, having two different diameters of 5.54 mm and 3.90 mm. Cladding materials are FC92 and HT9. RE contains Nd, Ce, Pr, and La. It is also intended to confirm the role of the Cr barrier at a higher temperature. The fuel rodlets having the diameter of PGSFR fuel are placed in the upper part of the rig. The SMIRP-2 irradiation rig and rodlets were fabricated and ready to be irradiated.

Since HANARO is a thermal test reactor, it is required to verify irradiation performance of PGSFR fuel rods under the fast neutron condition. An integral test of fuel rods having FC92 as well as HT9 claddings is being performed in BOR-60. The test fuel rods have the dimensions identical to those of PGSFR fuels except for their length. An irradiation rig accommodates seven fuel rods. Three fuel rods will be replaced by new ones at a peak local burnup of 3 at%. The remaining fuel rods continue to be irradiated up to a burnup of 7 at% to the end of 2019. The nominal peak cladding temperature of all fuel rods is targeted to reach 650°C. The fuel irradiation rig was fabricated, and its temperature verification was completed at an instrumented irradiation position of BOR-60. In-reactor behavior of the U–Zr fuel rod for the PGSFR initial core is scheduled to be confirmed most likely by 2020.

Irradiation test of U–TRU–Zr fuel is planned to start in 2018 in ATR (INL) by using TRU ingot produced through the pyroelectrochemical processing of the spent fuel.

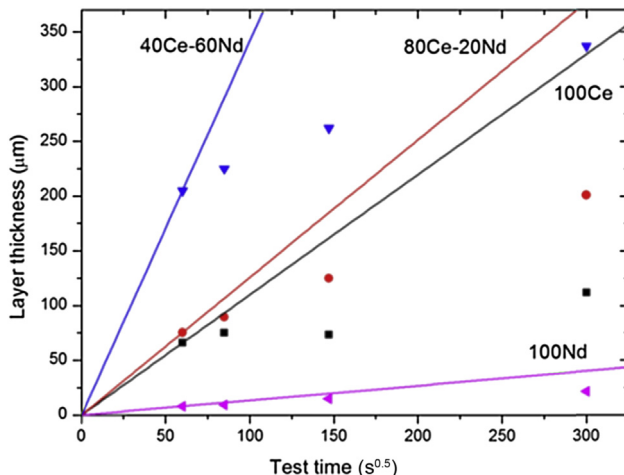


Fig. 19 – Diffusion couple test results of HT9 cladding with rare earth alloys.

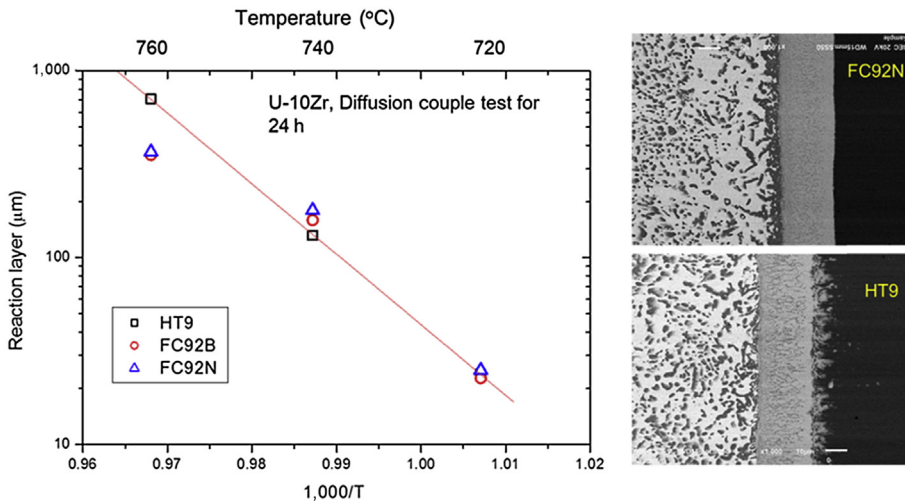


Fig. 20 – Diffusion couple test results of FC92 cladding with U–Zr metal fuel.

In addition to the in-pile tests, it is indispensable to make fuel verification under out-of-pile as well as whole pin furnace test and FCCI test.

High-temperature heating tests were performed with the SMIRP-1-irradiated fuels. First test series were run for U–10Zr/T92 specimen (750°C , 1 h) and U–10Zr–5Ce/T92 specimen (800°C , 1 h) [27]. Heating rate to the target temperature was $0.2^{\circ}\text{C}/\text{s}$. The experiment was conducted under helium environment.

As shown in Fig. 18, the eutectic melting region was locally observed in the case of the U–10Zr/T92 specimen. However, in the case of the U–10Zr–5Ce/T92 specimen, the eutectic melting region was not found, because there was a small gap between the fuel slug and cladding, which were present after the completion of the SMIRP-1 test, and the gap was sustained during the test. The eutectic melting region of the U–10Zr/T92 specimen exhibited that the U element from the fuel preferentially penetrated into the cladding, but Fe from the cladding moved slightly into the fuel region. It was also observed that the Nd fission product diffused into the cladding. The maximum penetration depth was measured to be $115\ \mu\text{m}$, from which the penetration rate was calculated. This penetration rate of $0.032\ \mu\text{m}/\text{s}$ is almost close to the value ($0.026\ \mu\text{m}/\text{s}$) predicted by an existing correlation for fuel design.

The effect of rare earth on FCCI behavior was examined by performing the out-of-pile diffusion couple test. A multi-component rare earth alloy (Nd–Ce–Pr–La) that simulates

fission products was prepared, and then the diffusion couple test along with HT9 was performed.

Compared with a single rare earth element, the multi-component alloy increased the thickness of the interaction layer [28]. To investigate the alloying element quantitatively, binary model alloys ($x\text{Ce} - y\text{Nd}$) were prepared. It showed that the reaction thickness of some alloys (40Ce–60Nd) was five times higher than that expected. Furthermore, FCCI tests were conducted under the situation that the rare earth alloy was arranged between the fuel and the cladding layers, as shown in Fig. 19. The presence of the rare earth layer enhanced the FCCI considerably, indicating that such synergism is required to be investigated more systematically.

A comparative study has been conducted on the FCCI behavior of FC92 relative to HT9. A diffusion couple test has been carried out with U–10Zr fuel at temperatures of 720°C , 740°C , and 760°C . It was revealed that FC92 cladding materials showed FCCI behavior similar to that of HT9, as presented in Fig. 20. Further out-of-pile diffusion couple tests are required to accumulate FCCI data for wider compositions of metal fuel as well as rare earth materials. The FCCI test results for un-irradiated fuel will be analyzed in connection with the transient test results of an irradiated fuel rod.

Out-of-pile tests of the PGSFR fuel assembly are under way. A full-size test fuel assembly was fabricated as shown in Fig. 21. Fig. 22 shows a layout of the fuel assembly test facility where test equipment is being installed. Fuel assembly

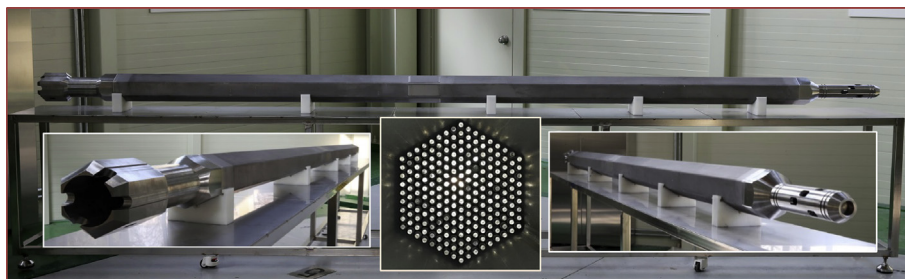


Fig. 21 – PGSFR fuel assembly. PGSFR, prototype generation-IV sodium-cooled fast reactor.

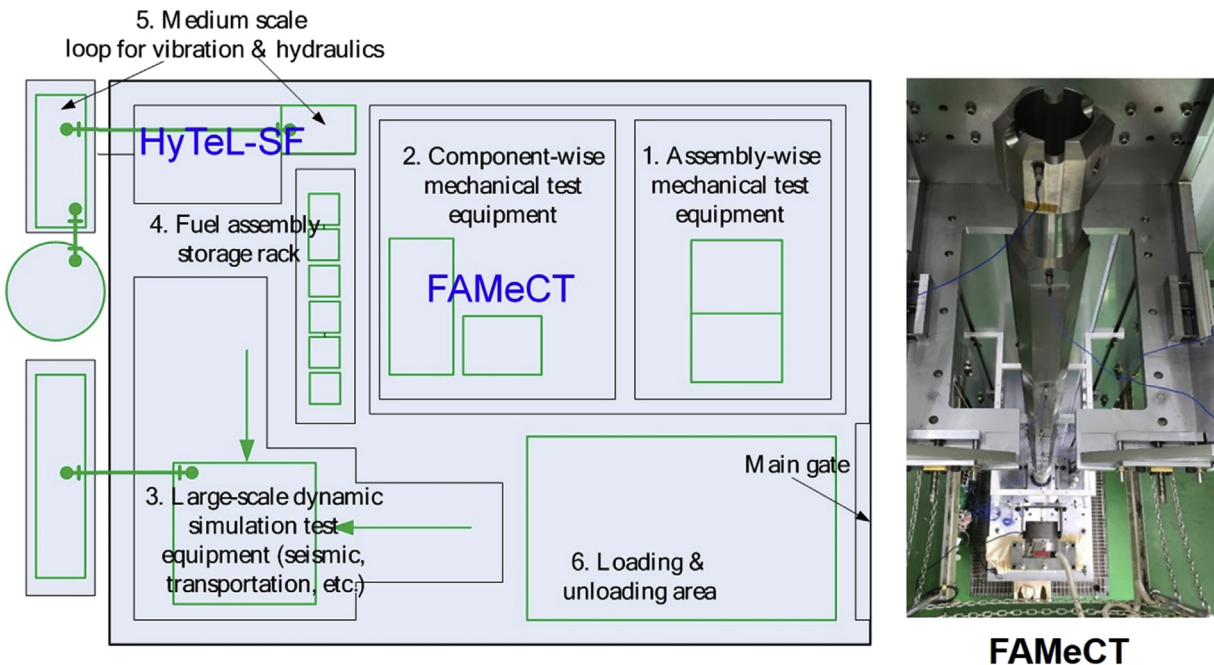


Fig. 22 – Fuel assembly test facility. HyTeL-SF, hydraulic test loop for sodium-cooled fast reactor fuel; FAMeCT, fuel assembly mechanical characterization tester.

mechanical tests are conducted in the assembly-wise mechanical characterization tester, called FAMeCT, in air at room temperature. A dynamic simulator is used to test a response of the fuel assembly under seismic conditions. Bending stiffness, vibration characteristics, and impact properties in vertical as well as horizontal directions are measured.

The hydraulic test loop for SFR fuel is under preparation for the fuel assembly hydraulic test in water. The test loop accepts a full-scale fuel assembly. The hydraulic test loop for SFR fuel consists of a main circulation pump, a water storage tank, a flow meter, a flow control valve, a heat exchanger, and a cooling tower. The coolant conditions of water will be matched to that of sodium in terms of Reynolds number.

3. Summary

Metal fuels, U–Zr and U–TRU–Zr, are being developed for the PGSFR to be built by 2028. U–Zr fuel is a driver for the initial core of the PGSFR, and TRU fuel will gradually replace U–Zr fuel after its qualification in the PGSFR. For U–Zr fuel, fuel design for the PGSFR, and fabrication of all the fuel components and fuel assembly were performed. Verification tests of U–Zr fuel are under way. U–TRU–Zr fuel uses TRU recovered through the pyroelectrochemical processing of spent PWR fuels, which contain highly radioactive minor actinides and chemically active lanthanide elements as carryover impurities. An advanced fuel slug casting system that can prevent vaporization of volatile elements through control of the atmospheric pressure of the casting chamber, and also deal with chemically active lanthanide elements by using protective coatings in the casting crucible, was developed. The fuel cladding of FM steel, FC92, which has a higher mechanical

strength at a high temperature than conventional HT9 cladding, was developed and fabricated, and is being irradiated in the fast reactor. A barrier such as Cr electroplating on the inner cladding surface to prevent an interaction between the metal fuel and cladding during irradiation was fabricated and tested in the reactor, showing satisfactory performance.

As the first milestone, performance of U–Zr fuel will be verified, and technical feasibility of TRU fuel fabrication and performance will be demonstrated by 2020. Then, the qualified metal fuel will be supplied to the PGSFR to be built by 2028.

Conflicts of interest

All authors have no conflicts of interest to declare.

Acknowledgments

This work was supported by the Nuclear Research & Development Program of the National Research Foundation (NRF) grant (2012M2A8A2025646) funded by the Korean government (Ministry of Science, ICT and Future Planning).

REFERENCES

- [1] GIF-005–00, Generation IV Roadmap, R&D scope report for liquid-metal-cooled reactor systems, December 2002.
- [2] H. Lee, G.-I. Park, K.-H. Kang, J.-M. Hur, J.-G. Kim, D.-H. Ahn, Y.-Z. Cho, E.H. Kim, Pyroprocessing technology development at KAERI, Nucl. Eng. Technol. 43 (2011) 317–328.
- [3] Y.-I. Chang, Technical rationale for metal fuel in fast reactors, Nucl. Eng. Technol. 39 (2007) 161–170.

- [4] D.C. Crawford, D.L. Porter, S.L. Hayes, Fuels for sodium-cooled fast reactors: US perspective, *J. Nucl. Mater.* 371 (2007) 202–231.
- [5] J. Carmack, K.O. Pasamehmetoglu, D. Alberstein, Assessment of startup fuel options for the GNEP Advanced Burner Reactor (ABR), INL/EXT-08–13773.
- [6] OECD Nuclear Energy Agency (NEA), State-of-the-art report on innovative fuels for advanced nuclear systems, NEA No. 6895, 2014.
- [7] T. Sofu, A review of inherent safety characteristics of metal alloy sodium-cooled fast reactor fuel against postulated accidents, *Nucl. Eng. Technol.* 47 (2015) 227–239.
- [8] D.E. Burkes, R.S. Fielding, D.L. Porter, D.C. Crawford, M.K. Meyer, A US perspective on fast reactor fuel fabrication technology and experience part I: metal fuels and assembly design,, *J. Nucl. Mater.* 389 (2009) 458–469.
- [9] K.H. Kim, H. Song, S.J. Oh, J.W. Lee, J.Y. Park, C.B. Lee, Fabrication and quality inspection of U–10wt.%Zr fuel rod for irradiation test, Proceeding of the Transactions of the Korean Nuclear Society Spring Meeting, Jeju, Korea, May 2016, pp. 11–13.
- [10] C.L. Trybus, Injection casting of U–Zr–Mn, surrogate alloy for U–Pu–Zr–Am—Np, *J. Nucl. Mater.* 224 (1995) 305–306.
- [11] S.W. Kuk, K.H. Kim, J.H. Kim, H. Song, S.J. Oh, J.Y. Park, C.B. Lee, Y.S. Youn, J.Y. Kim, Phase characteristics of rare earth elements in metallic fuel for a sodium-cooled fast reactor by injection casting, submitted.
- [12] J.H. Kim, J.W. Lee, K.H. Kim, C.B. Lee, Preliminary study on the fabrication of particulate fuel through pressureless sintering process, *Sci. Technol. Nucl. Install.* 2016 (2016) 7, 3717361, <http://dx.doi.org/10.1155/2016/3717361>.
- [13] R.B. Baker, F.E. Bard, R.D. Leggett, A.L. Pitner, Status of fuel, blanket, and absorber testing in the fast flux test facility, *J. Nucl. Mater.* 204 (1993) 109–118.
- [14] J.S. Cheon, C.B. Lee, B.O. Lee, J.P. Raison, T. Mizuno, F. Delage, J. Carmack, Sodium fast reactor evaluation: core materials, *J. Nucl. Mater.* 392 (2009) 324–330.
- [15] Y. Yano, S. Yamashita, S. Ohtsuka, T. Kaito, N. Akasaka, T. Shibayama, S. Watanabe, H. Takahashi, Mechanical properties and microstructural stability of 11Cr-ferritic/martensitic steel cladding under irradiation, *J. Nucl. Mater.* 398 (2010) 59–63.
- [16] A.A. Nikitina, V.S. Ageev, M.V. Leont'eva-Smirnova, N.M. Mitrofanova, I.A. Naumenko, A.V. Tselishchev, V.M. Chernov, Advances in structural materials for fast-reactor cores, *At. Energy* 119 (2016) 362–371.
- [17] T. Uwaba, S. Maeda, T. Mizuno, M.C. Teague, Study on the mechanism of diametral cladding strain and mixed-oxide fuel element breaching in slow-ramp extended overpower transients, *J. Nucl. Mater.* 429 (2012) 149–158.
- [18] International Atomic Energy Agency, Design, manufacturing and irradiation behaviour of fast reactor fuel, Proceedings of a technical meeting held in Obninsk, Russian Federation, 30 May–3 June 2011.
- [19] V.M. Troyanov, A.F. Grachev, L.M. Zabud'ko, M.V. Skupov, G.A. Kireev, Program and some results of pre-reactor studies of mixed uranium–plutonium nitride fuel for fast reactors, *At. Energy* 117 (2015) 236–242.
- [20] H. Kikuchi, K. Nakamura, T. Iwai, K. Nakajima, Y. Arai, T. Ogata, Establishment of technological basis for fabrication of U–Pu–Zr ternary alloy fuel pins for irradiation tests in Japan, *Trans. At. Energy Soc. Japan* 10 (2011) 323–331.
- [21] S.H. Kim, C.B. Lee, D. Hahn, Development of ferritic/martensitic steel for SFR fuel cladding tube, Nuclear fuels and structural materials for the next generation nuclear reactors (NFSM-II), Anaheim, USA, June 8–12, 2008.
- [22] T.K. Kim, J.H. Baek, C.H. Han, S.H. Kim, C.B. Lee, Effects of the fabrication process parameters on the precipitates and mechanical properties of 9Cr-2W-V-Nb steel, *J. Nucl. Mater.* 389 (2009) 359–364.
- [23] R.G. Pahl, C.E. Lahm, S.L. Hayes, Performance of HT9 clad metallic fuel at high temperature, *J. Nucl. Mater.* 204 (1993) 141–147.
- [24] W.J. Carmack, H.M. Chichester, D.L. Porter, D.W. Wootan, Metallography and fuel cladding chemical interaction in fast flux test facility irradiated metallic U–10Zr MFF-3 and MFF-5 fuel pins, *J. Nucl. Mater.* 473 (2016) 167–177.
- [25] J.S. Cheon, K.H. Kim, S.J. Oh, J.H. Kim, C.T. Lee, B.O. Lee, C.B. Lee, U–Zr SFR fuel irradiation test in HANARO, IAEA Technical Meeting on Design, Manufacturing and Irradiation Behaviour of Fast Reactors Fuels, Russia, 2011.
- [26] J.H. Kim, B.O. Lee, J.S. Cheon, S.H. Kim, Evaluation of material properties on the inner surface of Cr plated cladding tube for preventing fuel-cladding chemical interaction, 54 (2016) 855–861.
- [27] J.H. Kim, J.S. Cheon, B.O. Lee, J.H. Kim, H.M. Kim, B.O. Yoo, Y.H. Jung, S.B. Ahn, C.B. Lee, Results of high-temperature heating test for irradiated metallic fuel, in: Proceeding of the Korean Nuclear Society Autumn Meeting, Gyeongju, Korea, October 29–30, 2015.
- [28] J.H. Kim, J.S. Cheon, B.O. Lee, J.H. Kim, Interaction behavior between binary x Ce– y Nd alloy and HT9, *J. Nucl. Mater.* 479 (2016) 394–401.